VORTEX™ - A New High Performance Silicon Multi-cathode Detector for XRD and XRF Applications

Liangyuan Feng and Shaul Barkan,
Radiant Detector Technologies, LLC, 19355 Business Center Drive, Suite 8, Northridge, CA 91324
Jan S. Iwanczyk, Bradley E. Patt and Carolyn R. Tull,
Photon Imaging, Inc., 19355 Business Center Drive, Suite 8, Northridge, CA 91324

ABSTRACT

Vortex™, a high performance silicon multi-cathode detector, has been developed and extensively tested for potential x-ray diffraction (XRD) and x-ray fluorescence (XRF) applications. As a type of silicon drift detector, it utilizes our patented structure design [1] and achieves very low capacitance and very low leakage current with a relatively large active area (~50 mm^2). The detector operates at near room temperature with thermoelectric cooling and is thus very compact in size. These features make it ideal for many XRD and XRF applications. Results will be presented to demonstrate its superior performance over conventional cryogenic Si(Li) detectors, especially with respect to energy resolution and throughput at short amplifier peaking times.

Keywords: Vortex™, Silicon Multi-Cathode Detector, Silicon Drift Detector, FET, Peltier Cooler, X-ray Diffraction, X-ray Fluorescence, Multi-channel Analyzer, Single-channel Analyzer, Digital Pulse Processor, Sealed Proportional Counter, Graphite Monochromator, SMCD, SDD, XRD, XRF, Si(Li), SCA, MCA, DPP, SPC, FWHM, ICR, OCR

1. INTRODUCTION

The principle of silicon drift detectors (SDD) has been studied and reported since 1984 [2-7]. Starting from the mid-1990s, considerable efforts have been made toward fabrication of practical devices [5-11]. One of the important features of the SDD, compared with conventional planar detectors, is its extremely low capacitance (~0.06 pF) due to the unique structure and small anode size, virtually independent of the detector area. This feature makes it possible to fabricate large area, high performance detectors. The major advantages of the SDD include near room temperature operation (~ -70° C, which can be easily achieved using a standard Peltier cooler), compact size, and high throughput with good energy resolution at short peaking times. Our recent developments have resulted in a new type of SDD – the Vortex™ silicon multi-cathode detectors (SMCD) that have demonstrated significant improvements in performance as compared with earlier prototypes.

Analyzing the detector output with a properly optimized digital pulse processor (DPP), we can typically achieve energy resolutions of: 132 – 135 eV, 138 - 142 eV, 156 – 162 eV and 206 – 213 eV (FWHM at 5.9 keV) at peaking times of 12 μs, 4 μs, 1 μs and 0.25 μs, respectively. At a peaking time of 0.25 μs, the output count rate (OCR) can reach ~600 kcps at an input count rate (ICR) of ~1,500 kcps, which is fairly close to the calculated theoretical limit of 600 kcps at ICR = 1 Mcps. Furthermore, under such high input rates, there is virtually no loss in energy resolution and almost no shift in peak position. Such performances are unsurpassed by conventional cryogenic Si(Li) detectors. The excellent performance, plus its flexible, compact size and near room temperature operation make the Vortex™ detector ideal for many high-resolution, high-count rate XRD and XRF applications.

Conventional x-ray diffractometers use a sealed proportional counter (SPC) combined with a graphite monochromator to record diffraction patterns. We have measured a factor of 2.5 improvement in efficiency by replacing the SPC/graphite detection system with a Vortex™ detector. If a multichannel analyzer is used with the Vortex™, different diffraction patterns due to different x-ray tube lines (e.g. Cu K_α and Cu K_β) can be recorded simultaneously, which would otherwise take separate scans with the conventional XRD detection systems. For XRF applications, the Vortex™ detector can fit compactly into many areas where, for example, the detector size is of major concern or where liquid nitrogen supplies are limited. More importantly, as the Vortex™ detector has a large active area (~50 mm^2), it is particularly well suited for applications that require either a large solid angle or very high throughput. Other applications include fast x-ray elemental mapping that typically requires use of very short dwell times to record many full x-ray spectra. It is also an ideal x-ray detection device for many high flux synchrotron applications.

2. OVERVIEW

The Vortex™ silicon multi-cathode detector is hexagonal shaped with an active area of ~50 mm^2 and thickness of 350 - 400 μm. Figure 1 shows the backside of the detector, with the anode located at the center of ~80 μm in diameter, surrounded by multiple p^+ rings (the multi-cathode structure). The front side of the detector, composed of p^+ silicon, serves as the x-ray entrance window. The hexagonal shape allows for tight packing of multiple detector arrays as is desirable in some special applications. The detector is fabricated on high resistivity (2000-3000 ohm-cm) n-type silicon using state-of-the-art CMOS (complimentary metal-oxide-silicon) processing technology, based on our unique, patented structure design [1].

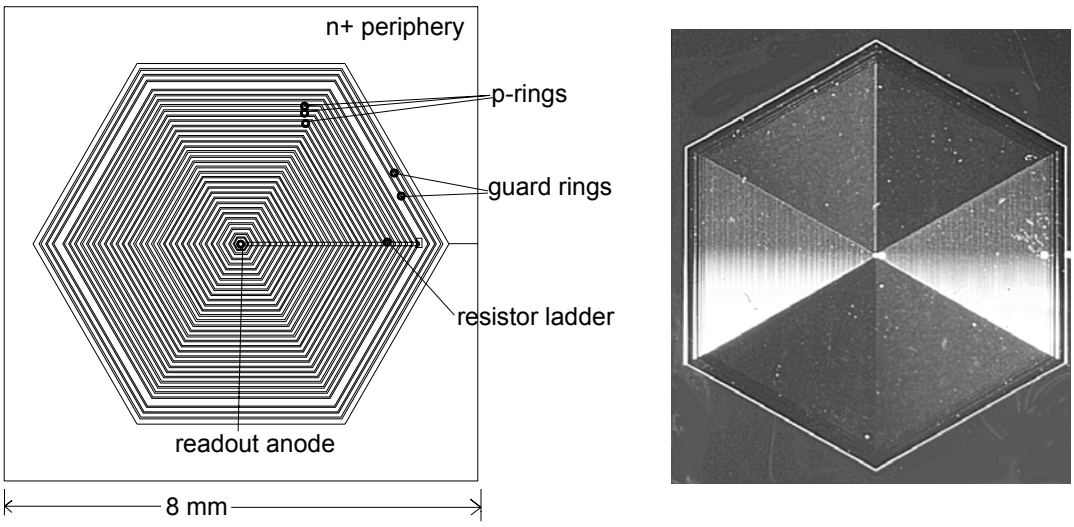

Figure 1. Basic structure of the Vortex™ silicon multi-cathode detector (left). A photo of the real detector diode is shown on the right, where the anode in the center and the multiple p^+ rings (the multi-cathode) are clearly seen.

The unique structure design, along with the processing techniques, ensure the achievement of extremely low capacitance (0.06 pF), very low leakage current (~10^{-9} A), and thus very low noise. When reverse-biased, the detector volume becomes fully depleted and, if the proper potential gradient is applied across the p^+ rings through the resistor ladder, a parabolic-shaped potential valley is produced within the detector volume forming a charge drift channel toward the tiny n^+ anode. The anode is connected to the input of a custom-designed, low noise, low capacitance FET (field effect transistor, the first amplification stage) bonded directly to the detector substrate using our unique patent-pending technology, which effectively reduces the overall input capacitance. The detector diode with FET is cooled with a 3-stage Peltier cooler to an operating temperature of about -70° C. The FET output is then fed to the input of a custom low noise preamplifier.

The detector noise arises mainly from two sources: the series noise due to the input capacitance and the parallel noise due to the leakage current. With increasing peaking time, the series noise decreases, but the parallel noise increases. At longer peaking times the noise is dominated by the parallel noise sources. In practice, the best energy resolution usually occurs between 4 – 12 μs. For the Vortex™ detectors there is typically no advantage in using peaking times greater than 12 μs. In fact, from throughput considerations, a shorter peaking time is always preferred.

Ignoring the negligible detector window absorption, the detector efficiency is close to 1 in the energy range of Cr K_α and Cu K_α photons (5.4 and 8.04 KeV, respectively) utilized by most XRD and XRF applications. At higher energies the efficiency drops rapidly as the photons penetrate through the detector volume. However, this is desirable in many applications since certain effects or interference due to high energy photons are eliminated. We have compared the detection efficiency of a custom-designed windowless Vortex™ detector with a windowless Si(Li) detector on an electron microscope at NIST, by measuring the ratio between the Cu L lines and Cu K_α line from a Cu sample under the same conditions. The ratio of Cu L/K_α was about 3 times higher for the Vortex™ detector compared with the Si(Li) detector, indicative of an extremely thin window on the Vortex™ device.

A photograph of a typical Vortex™ package is shown in Figure 2. The package dimensions are 169 x 68 x 65 mm, which is a convenient, portable size which will fit into most XRF and XRD systems. The detector package includes a vacuum-tight snout with a 25 μm thick Be window to accommodate the detector diode/cooler assembly, a cooler temperature regulator, a preamplifier and a heat exchange assembly. The detector components are vertically assembled in a manner so as to minimize microphonics and noise.

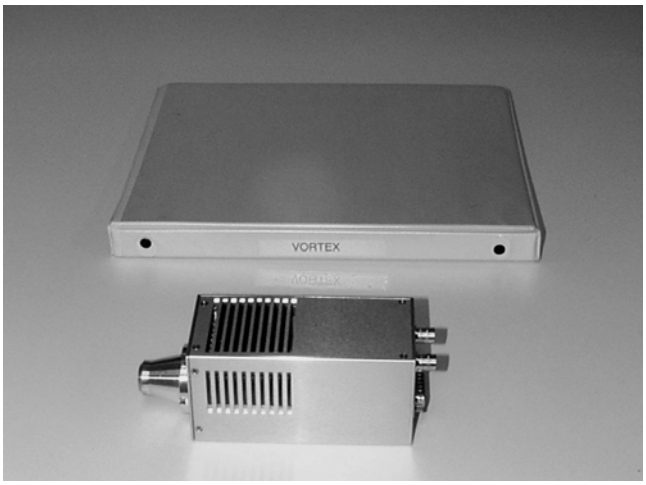

Figure 2. Photograph of the Vortex™ detector package, with a standard size manual folder shown for scale.

3. PERFORMANCE TESTS

The Vortex™ detectors have been extensively tested in terms of energy resolution and throughput over a range of peaking times. In addition, we have also examined the count rate dependency of peak positions and resolution. In these tests, a DPP (model DXP-X10P from X-Ray Instrumentation Associates (XIA)) was used to characterize the detector response to various radioisotopes and x-ray tube sources. The DPP unit includes an analog signal conditioner, a digital shaping amplifier and an 8K multi-channel analyzer, along with necessary drivers for interfacing to a PC host via the standard parallel port. We have developed PI-SPEC^{TM} software which interfaces with the XIA DPP for spectrum acquisition and analysis. The DPP is properly optimized to maximize the throughput at short peaking times (<= 1 μs) with a small sacrifice in energy resolution. Figure 3 shows the energy resolution over a range of peaking times for the Vortex^{TM} detector compared with a 30 mm^2 Si(Li) detector. The Vortex™ detector has superior energy resolution compared with the 30 mm^2 Si(Li), and this is especially so at the short peaking times. Figure 4 shows the actual Fe^{55} spectra acquired at 12 μs and 1 μs peaking times with the Vortex^{TM} detector.

Tests were also conducted with the Vortex™ detector at short peaking times (<= 1 μs) and under very high input count rate s (ICR >= 1 MCPS). Figure 5 shows oscilloscope traces of the characteristic x-ray signals from a pure Cu foil irradiated with a Rh target x-ray tube, at a very short peaking time of 0.250 μs, under a range of input count rates. These traces show that the Cu K_α and Cu K_β signals remain clearly separated in amplitude at very high input rates (up to 1 MCPS). Figure 6 shows the actual Cu spectra acquired at different count rates. It should be noted that there is only a 6 eV change in resolution and a 1 eV change in peak position, when the input count rate changes from 25 kcps to 1 Mcps. As can be seen, the Cu K_α and Cu K_β lines are fully separated at this short peaking time and high input count rate. The graphs in Figure 7 show the output count rate as a function of input count rate, and the peak position and energy resolution shift as a function of count rate for the Vortex™ detector. At 0.25 μs peaking time, the OCR is greater than 600 kcps at an input rate of ~1.5 Mcps. Moreover, there are only minor changes in the Cu K_α energy resolution and virtually no change in the Cu K_α peak position when the ICR reaches 1 Mcps.

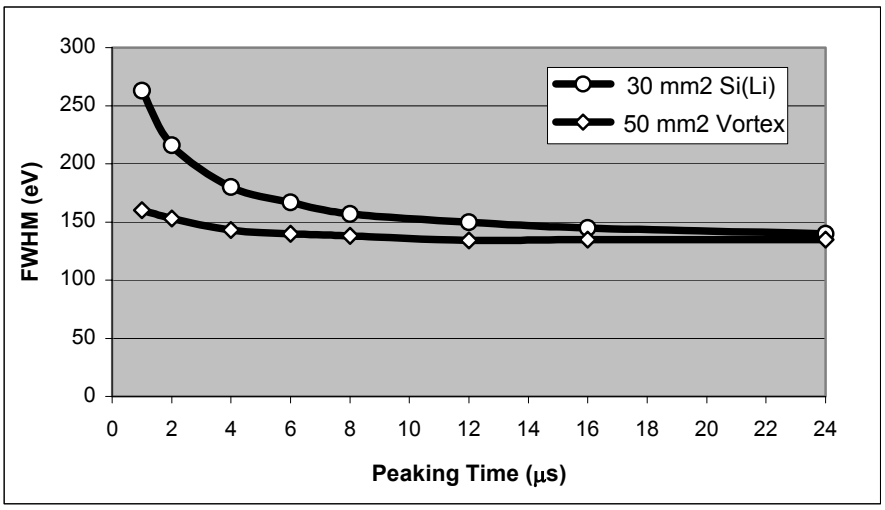

Figure 3. Comparison of energy resolution of the 30 mm^2 Si(Li) and the 50 mm^2 Vortex™ detectors over a range of peaking

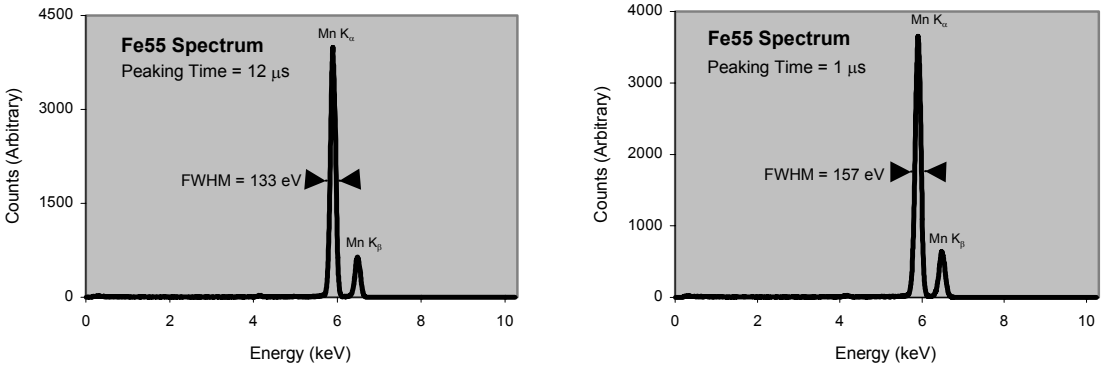

Figure 4. Fe^{55} spectra acquired using the Vortex™ detector at 12 μs (left) and 1 μs (right) peaking times.

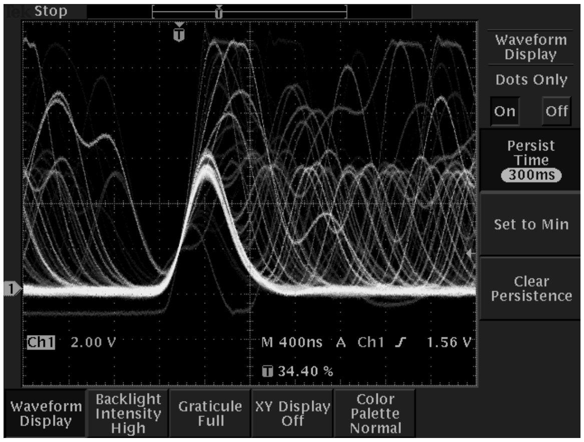

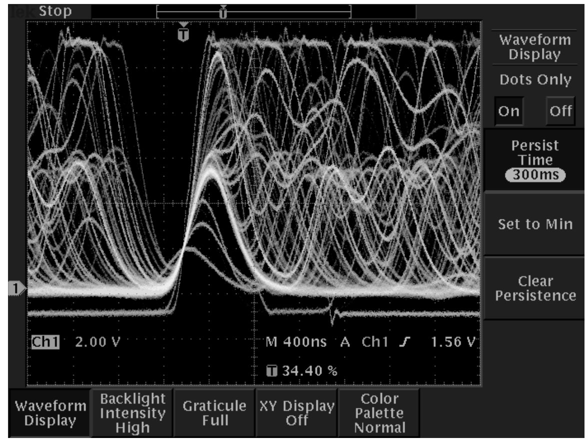

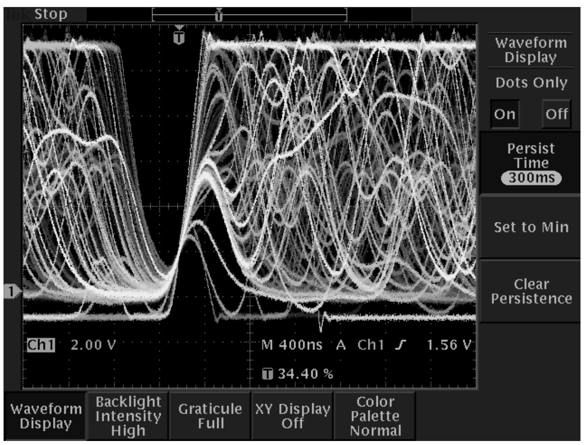

Figure 5. Oscilloscope traces of characteristic x-ray signals from a pure Cu foil irradiated with a Rh target x-ray tube, at a peaking time of 0. 25 μs. The amplitude separation of the Cu K_α and Cu K_β signals is clearly seen.

Input Count Rate (ICR):

Upper-left	:	500 kcps
Upper-right	:	800 kcps
Left	:	1 Mcps

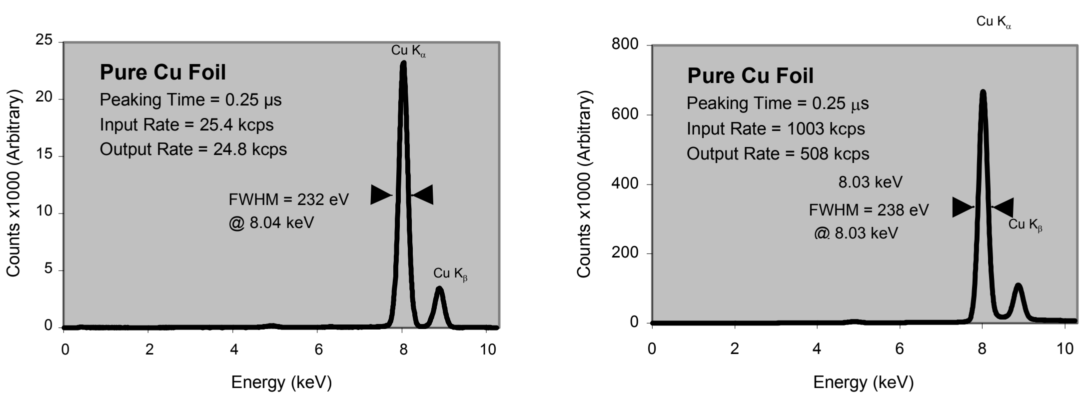

Figure 6. Cu spectra acquired using 0.25 μs peaking time at ICR = 25.4 kcps (left) and ICR=1003 kcps (right).

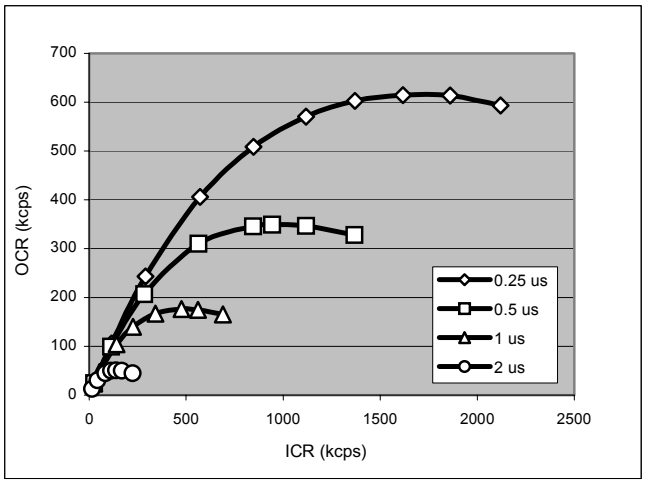

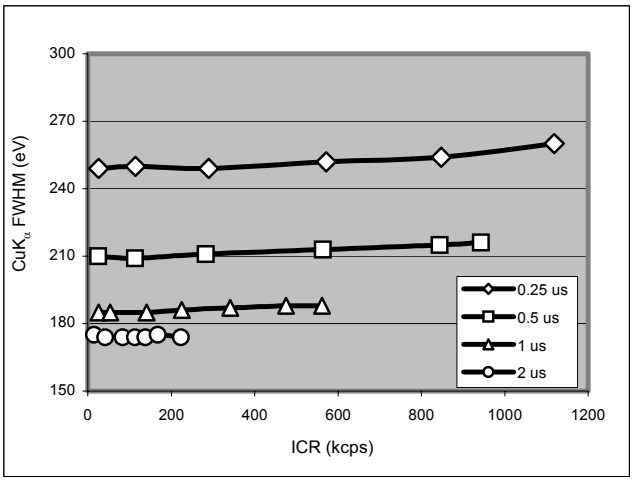

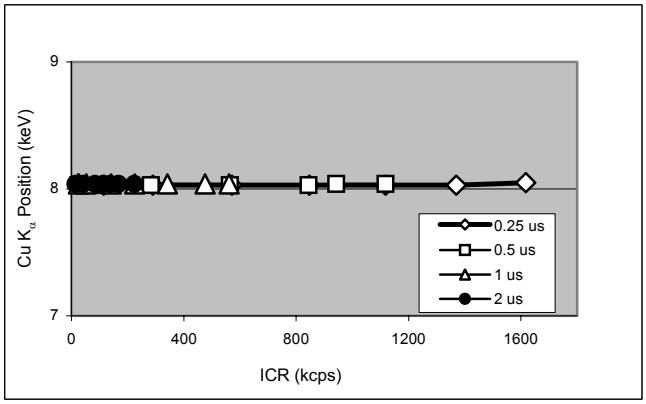

Figure 7. Vortex™ detector performance at short peaking times. Data were obtained using an optimized DPP from XIA and the Photon Imaging PI-Spec™ software. Signals were from a pure Cu foil irradiated with a Rh target X-ray tube.

Upper-left: Throughput chart (OCR vs. ICR)
Upper-right: Cu K_α FWHM vs. ICR
Left: Cu K_α position vs. ICR

4. TESTS ON X-RAY DIFFRACTOMETERS

Traditional high resolution x-ray diffractometers use a sealed proportional counter (SPC) in conjunction with a graphite monochromator to achieve separation of characteristic diffraction patterns due to different diffracting lines such as Cu K_α and Cu K_β from the Cu x-ray tube. The associated read-out electronics are typically an SCA (Single Channel Analyzer) plus a scaler. In a join effort with NIST, we installed a Vortex™ detector on one of their x-ray diffractometers to replace the SPC/graphite detection system. Several samples were tested, including a single crystal silicon wafer and a SiO_2 powder sample. An XIA DPP was used in conjunction with a modified version of our PI-Spec™ software to read out the Vortex™ output. The modified software allows the read out of predefined ROI (region of interest) counts in very short time intervals ranging from 0.1 to 10 seconds. Figure 8 shows comparative diffraction plots from a single crystal Si (100) wafer sample obtained with both the SPC/graphite and the Vortex™ detector systems. In the experiment, the Cu anode x-ray tube was operated at 40 kV/50 mA and a 5 mm / 10 mm slit combination was used in front of the tube. The scan was taken for a duration of 300 seconds for each plot, with the scan range between 67 and 72 degrees. Each point of the scan is represented by the counts integrated over the Cu K_α ROI window within a 1 second interval. The Cu K_α ROI bounds were selected to be 7.75 keV and 8.32 keV. A peaking time 0.25 μs was used for the DPP processing to maximize the output counts. The difference of the plots indicates that the use of the Vortex™ detector system resulted in an improvement in detection efficiency by a factor of ~2.5 as compared with the SPC/graphite system. An additional advantage of using the Vortex™ detector is that the spectral background of the measurements is much lower, which could lead to lower detection limits of the diffraction peaks.

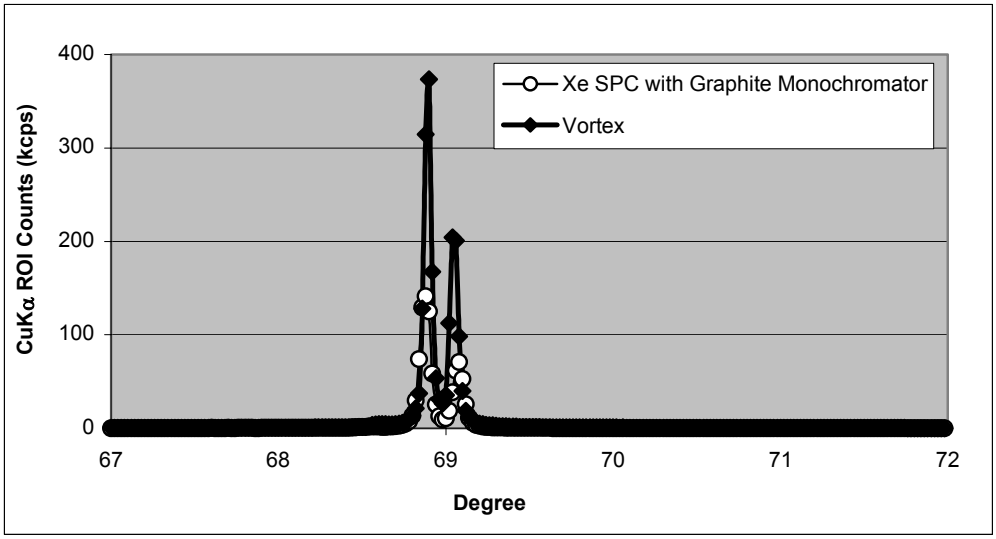

Figure 8. Comparison of diffraction plots taken with a conventional SPC/graphite monochromator and a Vortex™ detector on the NIST XRD instrument. The Vortex™ detector is 2.5 times more efficient than the SPC/graphite monochromator system.

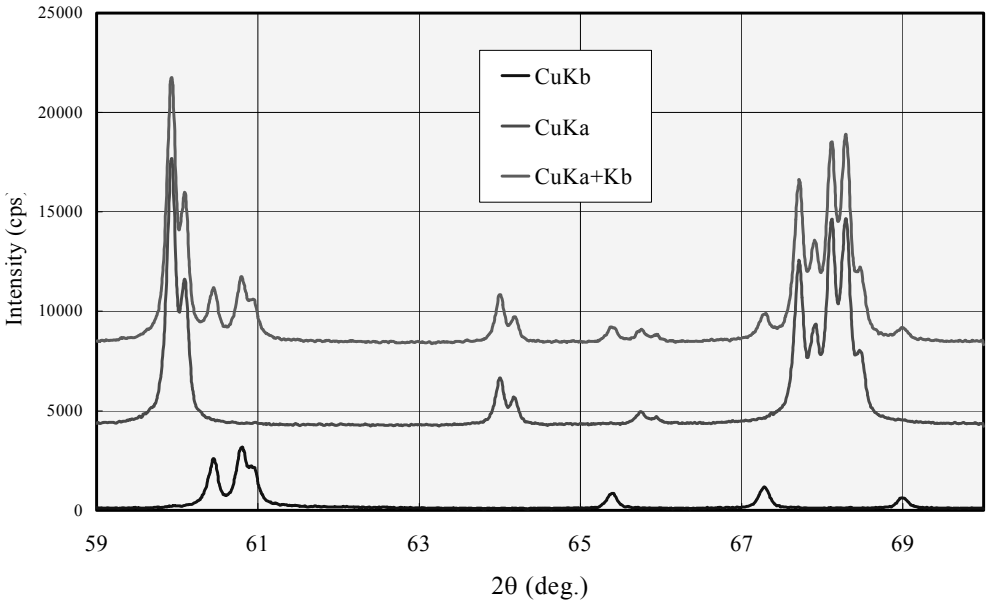

Figure 9. Quartz powder diffraction patterns obtained using the Vortex™ detector in place of the SPC/graphite detection system. (Courtesy of Rigaku, Inc.)

The Vortex™ detector was also tested at Rigaku, Inc. on an x-ray diffractometer. A quartz powder sample was scanned for its diffraction patterns from the Cu K_α and Cu K_β tube lines. The readout electronics included an SCA plus a scaler. In Figure 9, the curve on the top was obtained by setting the SCA to accept both the Cu K_α and Cu K_β lines. The middle and the bottom curves were obtained by setting the SCA to accept the Cu K_α only, and the Cu K_β only, respectively. As can be seen in this figure, the Cu K_α doublet generates the so-called five-finger pattern, but the Cu K_β as a singlet generates a much simpler and cleaner pattern which is naturally much more desirable. However, these patterns were obtained from multiple scans. Since the Vortex™ detectors have sufficient energy resolution to separate the Cu K_α and Cu K_β lines, it is optimal to use an MCA (Multi-Channel Analyzer) as the read-out electronics. The obvious advantage of using an MCA, such as the XIA DPP used in

the test shown here, is that all these patterns can be recorded from just one shot of the scan. Unfortunately, in this particular measurement, an MCA was not used.

5. CONCLUSIONS

The Vortex™ detectors have demonstrated great potential for use in XRD and XRF applications, due to their large active area, near room temperature operation and excellent x-ray performance. In particular, their extremely high throughput, good resolution, and virtually no peak shift and nor performance degradation with count rate make it very attractive for x-ray instrumentation which may include XRD systems, XRF portable and bench-top systems, elemental mapping microanalysis systems, and high flux synchrotron research systems.

ACKNOWLEDGEMENT

The authors acknowledge the support for this work received from U.S. Department of Commerce/NIST, Grant # SB1341-02-W-1074. This work was also supported in part by the DOE SBIR #DE-FG03-97ER82450, DOE SBIR #DE-FG03-99ER82853 and NIH SBIR #1R44-RR10647-02. The authors wish to thank Dr. Eric Steel of NIST and Dr. Jimpei Harada of Rigaku, Inc for their cooperation. Thanks also due to Dr. Valeri Saveliev, Ms. Elena Volkhonskaya, Mr. Jim Menjivar, and Mr. Jeffrey Combe at Radiant Detector Technologies for their technical assistance in various parts of this work.

REFERENCES

1. B.E. Patt, J.S. Iwanczyk, C.R. Tull and G. Vilkelis, US Patent # 6,455,858 B1
2. E. Gatti & P. Rehak, “Semiconductor Drift Chamber – An Application of a Novel Charge Transport Scheme”, Nucl. Instr. And Meth. In Phys. Res. 225 (1984) 608.
3. W. Chen, H. Kraner, Z. Li, P. Rehak, E. Gatti, A. Longni, M. Sampietro, P. Holl, J. Kemmer, U. Faschingbauer, B. Schmitt, A. Woner and J.P. Wurm, "Large Area Cylindrical Silicon Drift Detector", IEEE Trans. on Nucl. Sci. Vol. 39, No. 4, 1992, 619-628.
4. G. Bertuccio, A. Castoldi, A. Longoni, M. Sampietro and C. Gauthier, "New electrode geometry and potential distribution for soft X-ray drift detectors," Nucl. Inst. and Meth. in Phys. Res. A312 (1992) 613-616.
5. P. Jalas, A. Niemela, W. Chen, P. Rehak, A. Castoldi, A. Longoni, "New Results with Semiconductor Drift Chambers for X-ray Spectroscopy", IEEE Trans. on Nucl. Sci., V41, No.4 (1994) 1048.
6. E. Pinotti, A. Longoni, M. Gambelli, L. Struder, P. Lechner, C.V. Zanthier, & H. Kraner, “Room Temp. High Resolution X-ray Spectroscopy with Silicon Drift Chambers”, IEEE Trans. on Nucl. Sci., V42, No.1 (1995) 12.
7. J.S. Iwanczyk, B.E. Patt, G. Vilkelis, L. Rehn, J. Metz, B. Hedman & K. Hodgson, “Simulation and Modeling of a New Silicon Drift Chamber X-ray Detector Design for Synchrotron Radiation Applications”, Nucl. Instr. & Meth. in Phys. Res. A380 (1996) 288-294.
8. J. Segal, B.E. Patt, J.S. Iwanczyk, G. Vilkelis, J. Plummer, B. Hedman and K.O. Hodgson “A New Structure for Controlling Dark Current Due to Surface Generation in Drift Detectors,” Nucl. Instr. & Meth in Phys. Res A414 (1998) 307.
9. J.S. Iwanczyk, B.E. Patt, C.R. Tull, and L.M. MacDonald, “Novel x-ray and gamma-ray drift detectors based on silicon and compound semiconductors”, Proceedings of SPIE, Vol. 3768 (1999) 249-260.
10. J.S. Iwanczyk, B.E. Patt, C.R. Tull, J.D. Segal, C. Kenney, J. Bradley, B. Hedman, and K.O. Hodgson, “Large Area Silicon Drift Detectors for X-rays-New Results”, *IEEE Trans. Nucl. Sci*. Vol. 46, No. 3 (1999) 284-288.
11. J.S. Iwanczyk, Bradley E. Patt, Carolyn R. Tull, and Shaul Barkan, “High Throughput, Large Area, Silicon X-ray Detector for High Resolution Spectroscopy Applications”, Proceedings of the Microscopy and Microanalysis 2001 Conference, Long Beach, CA. Aug. 11-15, 2001.
12. M. Sampietro, L. Fasoli, P. Rehak and L. Struder, “Novel p- JFET embedded in silicon radiation detectors that avoids preamplifier feedback resistor”, IEEE Elect. Dev. Lett., 16 (1995) 208-210.
13. G. Cesura, N. Findeis, D. Hauff, N. Hornel, J. Kemmer, P. Klein, P. Lechner, G. Lutz, R. Richter and H. Seitz, “New pixel detector concepts based on junction field effect transistors on high resistivity silicon”, Nucl. Instr. Meth. A377 (1996) 521-528.
14. P.F. Manfredi, V. Re and V. Speziali, “Monolithic JFET preamplifier with nonresistive charge reset”, IEEE Trans. Nucl. Sci. 45 (1998) 2257-2260.
15. K. Misiakos and S. Kavadias, “A silicon drift detector with a p-type JFET integrated in the n-well anode”, Nucl. Instr. Meth. A458 (2001) 422-426.